Confined Water Clusters in a Synthetic Rubidium Gallosilicate with Zeolite LTL Topology

Yongjae Lee,*,† Sun Jin Kim,‡ Do-Cheon Ahn,§ and Nam-Soo Shin§

Department of Earth System Sciences, Yonsei University, Seoul 120-749, Korea, Nano-Materials Research Center, Korea Institute of Science and Technology, Seoul 136-791, Korea, and Pohang Accelerator Laboratory, Pohang University of Science and Technology (POSTECH), Pohang, 790-784, Korea

Received January 24, 2007. Revised Manuscript Received February 27, 2007

A rubidium gallosilicate with zeolite LTL framework topology has been synthesized under hydrothermal conditions, and the as-synthesized hydrated material was characterized via high-resolution synchrotron X-ray powder diffraction at room temperature. Rb-GaSi-LTL, $Rb_{9.8}Ga_{10.4}Si_{25.6}O_{72}\cdot 17.5H_2O$, is hexagonal, space group *P*6/*mmm*, with $a = 18.6260(1)$ Å and $c = 7.6459(1)$ Å. The framework model shows complete disordering of Ga and Si in the tetrahedral sites, which is analogous to the framework chemistry of its potassium counterpart, $K_{11}Ga_{10.3}Si_{25.7}O_{72}\cdot 15.1H_2O$ with $a = 18.5525(1)$ Å and $c = 7.5619(1)$ Å, but contrasts to the proposed preferential aluminum partitioning for the 6-ring sites in the aluminosilicate analogues. Similar to the cation distribution in the potassium analogue, half of the rubidium cations in the unit cell fully occupy the sites associated with the narrow channels on the $z = 1/2$ plane (sites B and C), whereas the other half fill, on average, five out of the six 8-ring sites in the recessed walls of the main 12-ring channel on the $z = 0$ plane (site D). All of the water molecules are located along the main 12-ring channels at $z = 0$, 1/6, 1/3, and 1/2 planes. Water molecules on the latter three planes form clusters within the 12-ring windows confinement via hydrogen bonding to one another and to framework oxygen atoms, while those on the $z = 0$ plane separate the water clusters by coordinating to the site D cations in the main channel. This partitioning of water molecules in the main channel becomes modulated in the hydrated potassium analogue and seems to be dependent on the chemistry of non-framework cations.

Introduction

It is important to have accurate structural understanding to fully utilize the chemical and physical properties of zeolites. The structures of as-synthesized zeolites are, however, often complicated because of partial occupancy and compositional disordering of either (or both) framework and non-framework species. Coupled to this, determination of non-framework contents distribution becomes further hindered when weakly bound water molecules behave like "fluid" in larger cavities and channels in more open pore zeolites, which are useful in various sorption and catalytic applications. It is also possible that these water molecules would not necessarily conform to the symmetry assumed for the framework.

Since its first synthesis in 1968 by Breck and Acara,[1] the structures of zeolite LTL were reported in various cationic forms and hydration status, such as hydrated (Na, K)-L,[2] hydrated (K, Ba)-G, L,[3] and dehydrated K-gallium L.[4] The LTL framework is composed of cancrinite cages (face symbol $4^6 6^3 6^2$ or $4^6 6^5$) stacked via 6-ring windows to form columns of alternating hexagonal prisms (face symbol $4^6 6^2$) and the cancrinite cages along the *c*-axis. These columns are connected by apical oxygen atoms of the cancrinite cages rendering larger circular 12-ring channels and smaller elliptical 8-ring channels along the *c*-axis. Unlike zeolite cancrinite, the main 12-ring channel is free from stacking faults and hence can serve as an important one-dimensional (1-D) reactor in chemical reactions and reservoirs for confined host−guest syntheses.[5−7]

In LTL zeolites, non-framework cations preferentially occupy the smaller cavities and channels at the center of the cancrinite cage (site B on $z = 1/2$ plane), in the middle of the elliptical 8-ring channel (site C on $z = 1/2$ plane) midway between adjacent cancrinite cages, and to a lesser extent, in the middle of the hexagonal prisms (site A on $z = 0$ plane).[2] These highly symmetric sites can host a maximum seven cations per topological unit cell in *P*6/*mmm*, and any remaining cations are to be found in the main channels near the boat-shaped 8-ring sites on $z = 0$ planes. These cations in the main channels are assumed to be coordinated by water molecules in hydrated forms and hence readily exchangeable.[8−10] Such partitioning of non-framework cations into the narrow cavities and channels requires a variable amount of water

† Yonsei University.
‡ Korea Institute of Science and Technology.
§ Pohang Accelerator Laboratory.

(1) Breck, D. W.; Acara, N. A. U.S. Patent 711,565, 1968.
(2) Barrer, R. M.; Villiger, H. *Z. Kristallogr.* **1969**, *128*, 352−370.
(3) Baerlocher, C.; Barrer, R. M. *Z. Kristallogr.* **1972**, *136*, 245−254.
(4) Newsam, J. M. *Mater. Res. Bull.* **1986**, *21* (6), 661−672.
(5) Jentoft, R. E.; Tsapatsis, M.; Davis, M. E.; Gates, B. C. *J. Catal.* **1998**, *179* (2), 565−580.
(6) Krueger, J. S.; Mayer, J. E.; Mallouk, T. E. *J. Am. Chem. Soc.* **1988**, *110* (24), 8232−8234.
(7) Newsam, J. M.; Silbernagel, B. G.; Garcia, A. R.; Hulme, R. *J. Chem. Soc., Chem. Commun.* **1987**, *9*, 664−666.
(8) Barrer, R. M.; Galabova, I. M. *Adv. Chem. Ser.* **1973**, *121*, 356−373.
(9) Dyer, A.; Amini, S.; Enamy, H.; Elnaggar, H. A.; Anderson, M. W. *Zeolites* **1993**, *13* (4), 281−290.
(10) Newell, P. A.; Rees, L. V. C. *Zeolites* **1983**, *3* (1), 22−27.

10.1021/cm070227u CCC: $37.00
Published on Web 04/06/2007

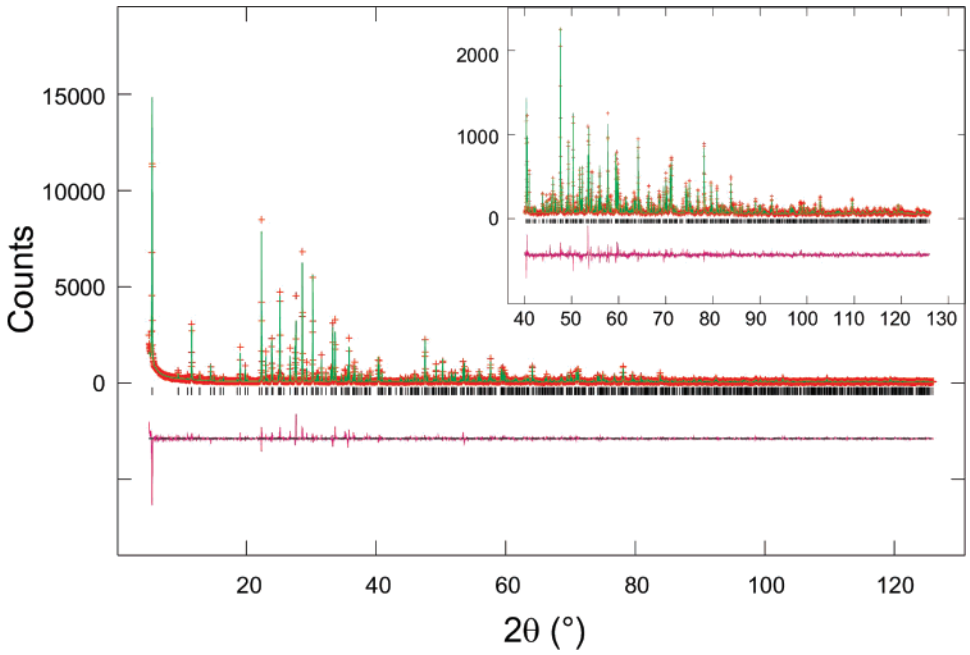

Figure 1. Final Rietveld fits between observed (dotted) and calculated (straight line) profiles for the hydrated Rb-GaSi-LTL. The difference curve is shown below in the same scale, and positions of contributing Bragg reflections are marked as vertical bars. A portion of the fit in the high 2θ region is shown as the inset.

molecules to form 1-D clusters exclusively in the main channel system.

Previous works on the structures of LTL zeolites lack description of hydrated forms for the reasons mentioned above and also due to the fact that non-framework cations synthesized or found in nature thus far have similar scattering powers and (or) bonding radii as water molecules; brief descriptions on cation−water coordinations are found in earlier literature.[3,11] To provide a detailed view of the separation of non-framework species into the channel systems in the LTL framework, a rubidium form of gallosilicate with zeolite LTL topology was synthesized, along with a potassium form, and the structures of the as-synthesized hydrated forms were analyzed using high-resolution synchrotron powder X-ray diffraction (XRD) and Rietveld refinement. Here, we report that water molecules form finite (or interrupted) columns with alternating hydrogen-bonded clusters and cation coordinated species along the main channels of the LTL framework.

Experimental Section

Synthesis and Initial Characterization. Rb-GaSi-LTL was synthesized using the hydrothermal method from a gel with the composition of 1.5:1.5:0.5:10:150 $Na_2O/Rb_2O/Ga_2O_3/SiO_2/H_2O$. A mixture of 0.938 g of Ga_2O_3 (Alfa, 99.99%), 1.24 g of NaOH (Aldrich, 97%), 3.72 g of RbOH (Alfa, 82.5%), and 16.7 g of water was heated at 110 °C for 16 h in a Teflon bottle. After cooling to room temperature, 15 g of colloidal silica (Ludox AS 40, Aldrich) was added to the above solution while stirring. After 24 h, the resultant gel was transferred into a Teflon lined vessel and heated at 110 °C for 10 days. The product was recovered by filtration, washed with deionized water, and dried at 100 °C. K-GaSi-LTL was synthesized from the same procedure as that of Rb-GaSi-LTL but using an initial gel with the composition of 1.5:0.5:5.0:80 $K_2O/Ga_2O_3/SiO_2/H_2O$.

(11) Artioli, G.; Kvick, A. *Eur. J. Mineral.* **1990**, *2* (6), 749−759.

Table 1. Crystallographic Data from Structure Refinements of the Hydrated Rb-GaSi-LTL and the Hydrated K-GaSi-LTL[a]

	Rb-GaSi-LTL	K-GaSi-LTL
unit cell formula	$Rb_{9.82(1)}Ga_{10.45}Si_{25.55}O_{72}\cdot 17.5(3)H_2O$	$K_{10.14(2)}Ga_{10.25}Si_{25.75}O_{72}\cdot 15.5(2)H_2O$
formula weight	3752.24	3265.06
space group	*P*6/*mmm*	*P*6/*mmm*
unit cell dimensions (Å)	$a = 18.6260(1)$	$a = 18.5525(1)$
	$c = 7.6459(1)$	$c = 7.5619(1)$
volume (Å^3)	2297.21(2)	2254.07(1)
profile coefficients (GU, GV, GW, LX, LY, S/L, H/L)	15, −3, 1.38, 2.81, 0, 0.01, 0.01	15, −3, 0.37, 1.24, 2.83, 0.01, 0.01
calculated density (g/cm^3)	2.687	2.383
number of peaks	790	776
restraints[b]/ parameters	20/60	20/60
reduced χ^2	3.07	2.47
R_{wp} (%)	15.5	14.1
R_{F2} (%)	13.7	10.7

[a] $[R_{wp}]^2 \equiv \sum\sigma i^{-2}(I_{obsd,i} - I_{calcd,i})^2/\sum\sigma i^{-2}(I_{obsd,i})^2$. $\chi^2 = [\sum\sigma_i^{-2}(I_{obsd,i} - I_{calcd,i})^2]/[N_{obsd} - N_{var}]$. [b] Tetrahedral geometrical restraints were constructed assuming complete disordering of Ga and Si in 2.44:1 and 2.51 ratios for the hydrated Rb-GaSi-LTL and K-GaSi-LTL samples, respectively. Overall weights (FACTR) of restraints were kept to 0.1 throughout the refinement.

Initial characterization of the bulk samples to verify phase identity, establish phase purity, and determine preliminary indexing was done by powder XRD using a Rigaku D/Max-IIA diffractometer. A step scan was performed over the 2θ range 3−50° with a step size of 0.02° and a step counting time of 3 s. No impurities were detected. Thermogravimetric analysis (TGA) measurements were carried out using a TA instrument (TGA2050) between room temperature and 1000 °C under a flowing N_2 atmosphere at a heating rate of 10 °C/min. Chemical analyses were performed by a Jarrell-Ash Polyscan 61E inductively coupled plasma (ICP) spectrometer and a Perkin-Elmer 5000 atomic absorption (AA) spectrophotometer. The Si/Ga and Rb/Ga ratios of Rb-GaSi-LTL were 2.44 and 0.87, respectively.

Table 2. Fractional Atomic Coordinates and Estimated Standard Deviations of Rb-GaSi-LTL (Upper Row) and K-GaSi-LTL (Lower Row)

atom	site	*x*	*y*	*z*	occupancy[a]	U_{iso}[b]
T4	12q	0.0947(1)	0.3578(1)	1/2	1	0.0144(3)
		0.0945(1)	0.3576(1)	1/2	1	0.0174(2)
T6	24r	0.1651(1)	0.4969(1)	0.2110(1)	1	0.0144(3)
		0.1659(1)	0.4977(1)	0.2118(1)	1	0.0174(2)
O1	6k	0	0.2718(4)	1/2	1	0.0204(7)
		0	0.2732(3)	1/2	1	0.0259(6)
O2	6m	0.1646(3)	0.3293(5)	1/2	1	0.0204(7)
		0.1648(2)	0.3295(4)	1/2	1	0.0259(6)
O3	12o	0.2654(2)	0.5308(3)	0.2510(6)	1	0.0204(7)
		0.2652(1)	0.5305(3)	0.2580(5)	1	0.0259(6)
O4	24r	0.1004(2)	0.4142(2)	0.3293(4)	1	0.0204(7)
		0.1004(2)	0.4119(2)	0.3230(3)	1	0.0259(6)
O5	12o	0.4249(1)	0.8498(3)	0.2643(6)	1	0.0204(7)
		0.4257(1)	0.8514(2)	0.2745(5)	1	0.0259(6)
O6	12p	0.1402(4)	0.4718(3)	0	1	0.0204(7)
		0.1454(3)	0.4788(3)	0	1	0.0259(6)
Rb2	2d	1/3	2/3	1/2	1	0.0336(4)
K2		1/3	2/3	1/2	1	0.0494(8)
Rb3	3g	0	1/2	1/2	1	0.0336(4)
K3		0	1/2	1/2	1	0.0494(8)
Rb4	6j	0	0.2950(1)	0	0.80(1)	0.0336(4)
K4		0	0.3050(2)	0	0.86(1)	0.0494(8)
W2	1b	0	0	1/2	0.69(3)	0.0336(4)
		0	0	1/2	0.26(2)	0.0494(8)
W3	6j	0	0.122(1)	0	0.35(1)	0.0336(4)
		0	0.122(1)	0	0.29(1)	0.0494(8)
W4	2e	0	0	0.153(2)	0.80(2)	0.0336(4)
		0	0	0.150(5)	0.32(2)	0.0494(8)
W5	12n	0	0.136(1)	0.328(1)	0.73(1)	0.0336(4)
		0	0.126(1)	0.327(1)	0.63(1)	0.0494(8)
W6	12p	0.098(1)	0.241(1)	0	0.36(1)	0.0336(4)
		0.097(1)	0.251(1)	0	0.44(1)	0.0494(8)

[a] Gallium occupancies for tetrahedral (T4 and T6) sites are fixed to 0.291 and 0.285 for Rb-GaSi-LTL and K-GaSi-LTL, respectively. [b] Isotropic displacement factors are constrained to be equal for tetrahedral atoms, framework oxygens, and non-framework species.

The sodium ions were detected by only very small amounts (<0.1%). The Si/Ga and K/Ga ratios of K-GaSi-LTL were 2.51 and 1.18, respectively.

Synchrotron Powder XRD Data Collection. High-resolution synchrotron powder XRD data of the hydrated Rb-GaSi-LTL and K-GaSi-LTL were measured at the 8C2 beamline of the Pohang Accelerator Laboratory. The incident X-rays were vertically collimated by a mirror and monochromatized to the wavelength of 1.5422(1) Å using a double-crystal Si(111) monochromator. The detector arm of the vertical scan diffractometer is composed of seven sets of soller slits, flat Ge(111) crystal analyzers, anti-scatter baffles, and scintillation detectors, with each set separated by 20°. Each specimen of approximately 0.2 g of powder was prepared by the flat plate side loading method to avoid the preferred orientation, and the sample was then rotated about the normal to the surface during the measurement to increase sampling statistics. A step scan was performed at room temperature from 5° in 2θ with 0.005° increments and 2° overlaps to the next detector bank up to 127° in 2θ.

The structural refinements were performed by Rietveld methods using the GSAS suite of programs[12,13] and the starting model of dehydrated gallium zeolite L by Newsam.[4] The background curve was fitted with a Chebyshev polynomial with 24 coefficients. The pseudo-Voigt profile function proposed by Thompson et al. was used to fit the observed peaks.[14] To reduce the number of parameters, isotropic displacement factors were refined by grouping the framework tetrahedral atoms, the framework oxygen atoms, and the non-framework cations and water oxygen atoms, respectively. Geometrical soft restraints on the T−O (T = Ga, Si) and O−O bond distances of the tetrahedra were applied: the distances between T−O were restrained to a target value of 1.663 ± 0.001 Å, and the O−O distances were restrained to 2.716 ± 0.005 Å, assuming the bond lengths for Si−O and Ga−O to be 1.61 Å and 1.82 Å, respectively, and their random occupation and linear variations with composition. Water molecules were located from difference Fourier synthesis at five different sites in the main channels and modeled using the oxygen scattering factor. In the final stages of the refinements, the weight of the soft restrain was reduced, which did not lead to any significant changes in the interatomic distances, and the convergence was achieved by refining simultaneously all background and profile parameters, scale factor, lattice constants, 2θ zero, atomic positional and thermal displacement parameters, and occupancy factors for water oxygen atoms. The Rietveld full-profile fit of Rb-GaSi-LTL is shown in Figure 1. The final refined parameters are summarized in Tables 1 and 2, and selected bond distances and angles are listed in Table 3.

Table 3. Selected Interatomic Distances (Å) and Angles (deg) of Rb-GaSi-LTL (Upper Row) and K-GaSi-LTL (Lower Row)[a]

T4−O1	1.689(3)	T4−O1−T4	129.5(4)
	1.668(3)		131.2(4)
T4−O2	1.635(2)	T4−O2−T4	147.3(6)
	1.628(2)		147.8(5)
T4−O4	1.645(3) × 2	T6−O3−T6	136.0(3)
	1.645(2) × 2		135.4(3)
av T4−O	1.654(2)[b]	T4−O4−T6	143.7(3)
	1.647(1)[b]		142.0(2)
T6−O3	1.674(2)	T6−O5−T6	147.0(3)
	1.663(2)		141.7(3)
T6−O4	1.669(3)	T6−O6−T6	147.8(4)
	1.669(3)		154.3(3)
T6−O5	1.664(2)	W2−W4	2.65(2) × 2
	1.674(2)		2.65(4) × 2
T6−O6	1.679(2)	W2−W5	2.86(1) × 12
	1.643(1)		2.68(1) × 12
av T6−O	1.672(1)[b]	W3−W3	2.27(3) × 2[c]
	1.662(1)[b]		2.26(3) × 2[c]
Rb2−O3	2.903(5) × 6	W3−W4	2.56(2) × 2[c]
K2−O3	2.853(4) × 6		2.53(3) × 2[c]
Rb3−O4	3.278(4) × 8	W3−W5	2.52(1) × 2[c]
K3−O4	3.313(3) × 8		2.48(1) × 2[c]
Rb3−O5	3.019(5) × 4	W3−W6	2.04(2) × 2[c]
K3−O5	2.934(4) × 4		2.16(2) × 2[c]
Rb4−O4	3.259(4) × 4	W3−W6	2.46(2) × 2[c]
K4−O4	3.110(3) × 4		2.67(1) × 2
Rb4−O6	3.011(6) × 2	W4−W4	2.34(3)[c]
K4−O6	2.996(5) × 2		2.27(7)[c]
Rb4−W3	3.22(3)	W4−W5	2.86(1) × 6
K4−W3	3.40(3)		2.70(2) × 6
Rb4−W6	2.50(2) × 2	W5−W5	2.53(1) × 2[c]
K4−W6	2.45(1) × 2		2.34(1) × 2[c]
Rb4−W6	3.27(2) × 2	W5−W5	2.63(1)
K4−W6	3.48(1) × 2		2.62(1)
W5−O1	2.85(1)	W6−W6	0.81(4)[c]
	3.02(1)		1.07(2)[c]

[a] Estimated standard deviations are in parentheses. [b] Standard deviations computed using $\sigma = 1/n[\sum_{i=1}^{n}\sigma i^2]^{1/2}$. [c] O−O distance shorter than 2.6 Å; simultaneous occupancy excluded or indicates partial (or disordered) hydrogen bonding.

Results and Discussion

The refined average T−O bond distance of 1.663(1) Å in the hydrated Rb-GaSi-LTL matches closely the expected

(12) Larson, A. C.; VonDreele, R. B. *GSAS; General Structure Analysis System*; Report LAUR 86-748; Los Alamos National Laboratory: Los Alamos, NM: 1986.
(13) Toby, B. H. *J. Appl. Crystallogr.* **2001**, *34*, 210−213.
(14) Thompson, P.; Cox, D. E.; Hastings, J. B. *J. Appl. Crystallogr.* **1987**, *20*, 79−83.

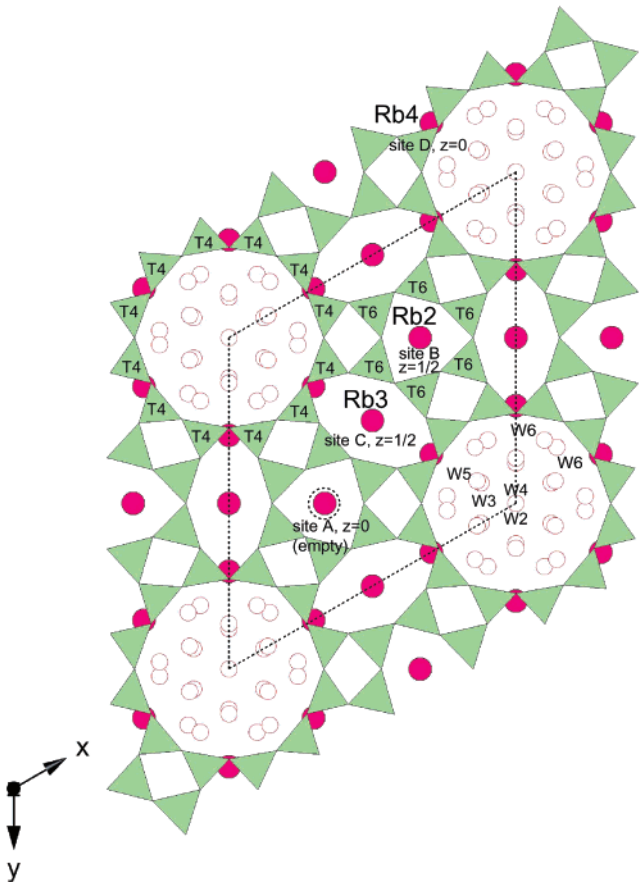

Figure 2. Polyhedral representation of Rb-GaSi-LTL viewed down [001] showing non-framework cations (filled circles) and water molecules (open circles). Tetrahedra are shown in the same color to illustrate the disordered distribution of gallium and silicon atoms at the 6-ring (T6) and 12-ring (T4) sites. Rubidium cation positions are marked with site labels and their respective heights along the *c*-axis. Site A in the middle of the 6-ring prism on the $z = 0$ plane is empty and shown as a dotted circle.

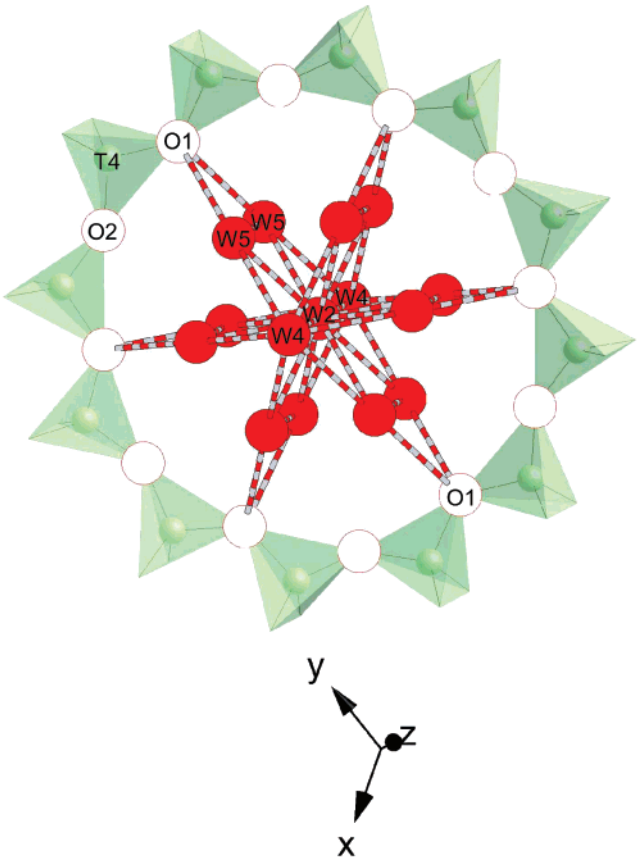

Figure 3. Illustration of a confined water cluster inside the 12-ring window on the $z = 1/2$ plane. Here, possible hydrogen bondings (banded bars) are shown to form between (water) oxygen atoms with interatomic distances in the range of 2.6−2.9 Å. The water cluster is held by bonding to framework O1 atoms, which define the access diameter of the 12-ring opening.

value from the random occupation of silicon and gallium at the tetrahedral sites in a 2.44:1 ratio, as derived from the chemical analysis (Table 3). Individual T−O distances, on the other hand, show some indication of gallium partitioning for the 6-ring T-sites as the average T6−O distance is larger than the average T4−O length (Table 3 and Figure 2). Similar trends were noticed in earlier studies where aluminum partitioning for the T6 site increased with decreasing Si/Al ratio.[2,3] For LTL zeolites containing large monovalent cations such as rubidium, however, the Si/Ga ratio would not decrease below 2.3 since rubidium cations are unlikely to occupy simultaneously the neighboring cancrinite cage (site B) and the double 6-ring site (site A; Figure 2). In addition, a reduction in symmetry and a doubling of the *c*-axis would be observed from the high-resolution powder diffraction data, were there an ordered Ga/Si distribution in our sample. Trial refinement using the subgroups of *P*6/*mmm* did not lead to convergence or meaningful interatomic distances. The observed distribution of T−O distances is therefore thought to be an analytical artifact as the 12-ring and 6-ring T-sites have different symmetry restrictions. For the hydrated K-GaSi-LTL model, the refined average T−O distances are smaller by a few σ than the corresponding values from the hydrated Rb-GaSi-LTL model, but in general, a similar conclusion for the framework model can be drawn. It is interesting to note the changes in the channel geometry upon the isomorphous gallium substitution. In the case of the hydrated Rb-GaSi-LTL, the free access diameter of the 12-ring channel (based on the opposite O1 atoms at $z = 1/2$) has expanded to ∼7.5 Å (on the basis of an oxygen ionic radius of 1.35 Å; Figure 3), compared to ∼7.1 Å in the hydrated (Na, K)-L,[2] whereas the largest free diameter inside the 12-ring channel (based on the opposite O6 atoms at $z = 0$) stays more or less the same to about 13 Å.

Rubidium cations are located at three different sites (Figure 2). Site B at the center of the cancrinite cage is fully occupied by Rb^+ ions as for site C on the same $z = 1/2$ plane midway between the centers of two neighboring cancrinite cages. These cations in the narrow cages and channels of the LTL framework bond to the framework oxygen atoms in 6-fold and 12-fold coordinations, respectively (Table 3). The remaining rubidium cations are found at site D on the $z = 0$ plane in the recess of the main channel walls (Figure 2). On the statistical basis from the refined fractional occupancy for site D cation, five out of six available 8-ring sites in each 12-ring cage are filled by rubidium cations. Unlike rubidium cations at sites B and C, site D cations can be accessed via the circular 12-ring openings as well as the elliptical 8-ring channel normal to the *c*-axis. In addition to the coordination by framework oxygen atoms, site D rubidium cations bond to water molecules at two different sites in the main channels (Table 3) and hence can be considered readily exchangeable.

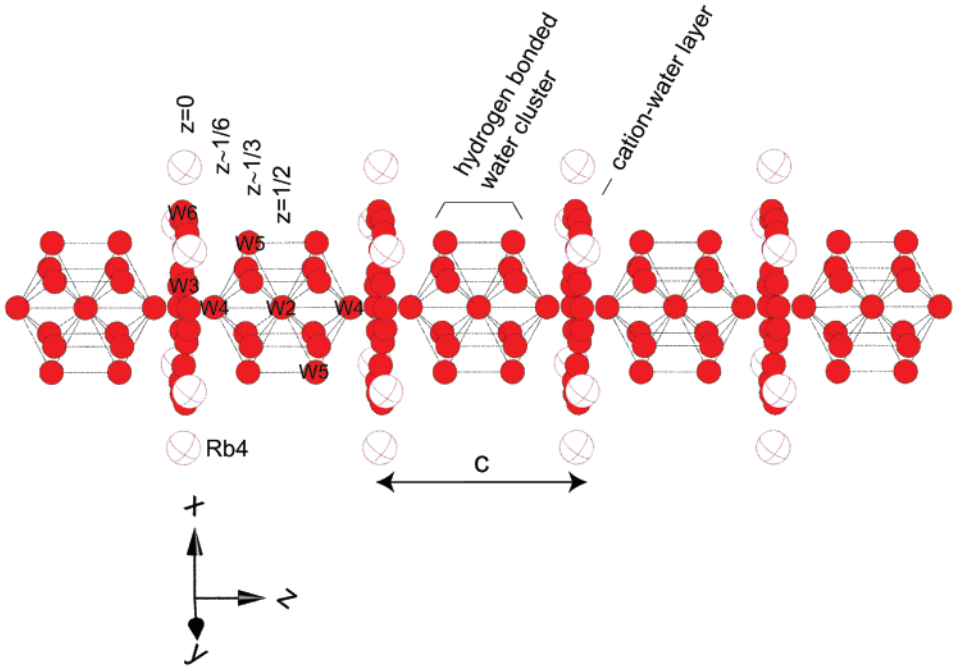

Figure 4. Non-framework contents inside the 12-ring channel of the hydrated Rb-GaSi-LTL, illustrating the alternation of hydrogen bonded (with bars) water clusters and cation−water layers along the *c*-axis. Oxygen atoms from water molecules are depicted by filled circles, and rubidium cations at site D (Rb4) are depicted by open circles. The Rb4 and water sites are not fully occupied. The arrow indicates the *c*-axis length.

Site A in the middle of the hexagonal prism is empty as was the case for the hydrated (K, Ba)-G, L[3] and the dehydrated K-gallium L.[4] The potassium cation distribution in the hydrated K-GaSi-LTL is similar to that of rubidium cation distribution in the hydrated Rb-GaSi-LTL, while site D in the former exhibits slightly higher population by potassium cations (Tables 2 and 3).

The refined water contents of the as-synthesized Rb-GaSi-LTL and K-GaSi-LTL are both in close agreement with those derived from the TGA; for Rb-GaSi-LTL, the total refined occupancy factors of water molecules account for 8.4 wt % and agree very well with the value of 8.3 wt % measured by TGA, and for K-GaSi-LTL, 8.5 wt % by XRD matches exactly to 8.5 wt % by TGA. As mentioned above, all of the water molecules are found exclusively in the main channels (Figure 2). These water molecules are rather "fixed" at five crystallographically distinct locations with varying degrees of site occupations and reasonably small thermal vibrations (though constrained to be the same as those of cations, see Table 2). In both models, the refined water positions can be approximated to $z = 0$, 1/6, 1/3, and 1/2 planes to constitute finite (or interrupted due to partial occupancies) columns along the *c*-axis. Intriguingly, three of the five water positions on the latter three planes (W2, W4, and W5) separate from the other two on the $z = 0$ plane (W3 and W6) and are confined within the 12-ring windows of the main channels (Figure 4). Though statistically populated by water molecules, these three sites resemble a cluster in the form of a bipyramidal hexagonal prism, which can be formed via hydrogen bonding between water molecules with oxygen interatomic distances in the range between 2.65(2) Å and 2.86(1) Å (Table 3). In the hydrated Rb-GaSi-LTL, this confined water cluster is held within the 12-ring window by orienting its columnar W5 oxygen atoms toward the O1 oxygen atoms of the 12-ring window with inter-oxygen distance of 2.85(1) Å (Figure 3). This might explain why the O1 oxygen atoms are drawn closer to the center of the 12-ring window than the O2 oxygen atoms, defining the free access diameter of the channel. On the other hand, water molecules at the W3 and W6 sites on the $z = 0$ plane do not form hydrogen bonding but coordinate to rubidium cations at site D in the main channel (Table 3). The water molecules in the main channel of the hydrated Rb-GaSi-LTL zeolite thus appear to partition into two alternating groups: the more populated, hydrogen-bonded water clusters interacting with the 12-ring confinement (Figure 3) and the weakly bonded, isolated water molecules dispersed in the large cavity midway between the 12-ring windows (Figure 4). This partitioning in spatial confinement and bonding character of water molecules seems to be modulated in the hydrated K-GaSi-LTL (Table 3); the interaction between the water cluster and the 12-ring window becomes weaker (the O1−W5 distance increases from 2.85(1) Å in Rb-GaSi-LTL to 3.04(1) Å in K-GaSi-LTL), whereas the hydrogen bondings within the cluster that are oriented toward the O1 oxygen of the 12-ring window becomes stronger (W2−W5 and W4−W5 distances decrease from 2.86 Å in Rb-GaSi-LTL to 2.68−2.70 Å in K-GaSi-LTL). This might be related to the different degrees of the overall hydration level upon non-framework cation substitution. Neutron diffraction studies would quantify the above proposed hydrogen-bonding models, and it would also be interesting to manipulate the water partitioning by controlled hydration via using either temperature or hydrostatic pressures.

Conclusion

To elucidate the non-framework cation−water partitioning in the channels of LTL zeolite, a rubidium form of gallosilicate was synthesized, and high-resolution synchrotron

powder XRD was used to derive an accurate structural model. Water molecules are located at well-defined positions along the main channel in two distinct groups: hydrogen-bonded water clusters about the plane of the 12-ring confinement and cation-coordinating water molecules sandwiching the clusters on the central plane of the 12-ring cages. Comparison to the non-framework model of the hydrated potassium gallosilicate analogue indicates that the water partitioning might be tailored via cation exchange and controlled hydration level.

Acknowledgment. This work was supported by the Korea Research Foundation Grant funded by the Korean Government (MOEHRD; KRF-2006-D00538). S.J.K. is grateful for the support from Korea Institute of Science and Technology (KIST). Experiments at PAL were supported in part by Ministry of Science and Technology (MOST) of the Korean Government and Pohang University of Science and Technology (POSTECH).

CM070227U